Effect of the Nature of Annealing Solvent on the Morphology of Diblock Copolymer Blend Thin Films

Rui Guo,[†] Haiying Huang,[†] Yongzhong Chen,[†] Yumei Gong,[†] Binyang Du,[‡] and Tianbai He*,[†]

State Key Laboratory of Polymer Physics and Chemistry, Changchun Institute of Applied Chemistry, Chinese Academy of Sciences, Changchun, 130022, P. R. China, and Key Laboratory of Macromolecular Synthesis and Functionalization, Department of Polymer Science & Engineering, Zhejiang University, Hangzhou, 310027, P. R. China

Received September 3, 2007; Revised Manuscript Received November 16, 2007

ABSTRACT: The morphologies and structures for the thin film of blend systems consisting of two asymmetric polystyrene-*block*-polybutadiene (SB) diblock copolymers induced by annealing in the vapor of different solvents, namely, cyclohexane, benzene, and heptane, which have different selectivity or preferential affinity for a certain block, were investigated by tapping mode atomic force microscopy (AFM) and transmission electron microscopy (TEM). The results revealed that even a slight preferential affinity of good solvent for one block would strongly alter the morphology of the blend thin film. An interesting structure of so-called "spheres-between-cylinders" ("sph-b-cyl") was obtained when annealing the blend thin film with a weight fraction ratio of 50/50 of the two components in the saturated vapor of cyclohexane, which is a good solvent for PB and a (near) Θ solvent for PS at 34.5 °C. The influence of the kinetic factors, such as the annealing time and vapor pressure of the solvent, together with the factors of the blend composition and the film thickness, on the morphology forming in the blend thin film systems was also investigated. Blending the block copolymers together with the solvent treatments is proved to be an effective way to control the structure and morphology of the thin films.

Introduction

Block copolymer, a special kind of soft matter, has attracted considerable attention of polymer chemists and physicists during the last few decades.[1−5] It is able to spontaneously form different kinds of well-ordered microdomain structures, which have potential applications in nanoscience and nanotechnology.[6−8] Various methods have been explored to control and manipulate the microdomain structures of the block copolymer.[3−5,9,10] Among these methods, synthesizing a precisely tailored block copolymer is considered to be a prominent route. Many novel structures of a block copolymer have been obtained by synthesizing complicated copolymers.[11] However, synthesis methods are sometimes complicated and costly. Alternatively, blending of two or more block copolymers offers a simple and economic way to control the structures of block copolymers. Special and desired morphologies, which are not accessible in the neat block copolymer system, can be obtained by this means.[12,13]

Various factors may have impact on the microdomain structures of the blend block copolymers. For example, for a binary blend of two AB diblock copolymers (α and β) with different block length, $(AB)_\alpha/(AB)_\beta$, there are at least six parameters which will influence the structures of the blend. They are the AB segment−segment interaction parameter χ, the degree of polymerization N_α and N_β, the volume fraction of the A block in the individual copolymers $f_{A,\alpha}$ and $f_{A,\beta}$, and the volume fraction of the α component in the blend Φ_α. Therefore, the blend block copolymers will have rich microdomain structures, depending on the mixing conditions.[14] Several reports have theoretically[15−18] and experimentally[19−26] depicted the rich structures of block copolymer mixtures in bulk. Meanwhile, only a few studies have paid attention to the morphologies and structures of the thin films of blend block copolymers.[27−30] A possible reason is that the factors determining the microdomain structures of block copolymers for thin films are much more complicated than that for bulk samples. For instance, the application of external fields,[31−42] solvent evaporation rate,[34,40−43] interaction of surface and interface,[35−37] and film confinement[40,42,44,45] might have significant effects on the morphology of the thin films.

In the present work, we focused on the morphology transition of the thin films of blend block copolymer (bcp) systems under solvent annealing treatment and investigated the effect of the nature of the annealing solvent on the morphology of blend thin films.

It is well-known that solvent-induced ordering has been exploited to control the microstructures of block copolymer thin films without thermal treatment.[38] Russell and co-workers[46] have obtained almost defect-free microstructures over large areas in the thin films of diblock copolymer/homopolymer blends by controlling the solvent annealing. We have extended such means of solvent treatment to the self-organization of PS-*b*-PMMA diblock copolymer blends in thin films.[30] After annealing in the vapor of a PMMA-selective solvent (acetone) for a certain time, a novel hexagonal packed circular multilayered structure has been obtained. Such interesting morphology was mainly induced by the selective interaction between the solvent acetone and the PMMA blocks. Does it still play an important role in the morphology of the blend bcp thin films if we alter the interaction of the polymer−solvent by changing the annealing solvent from a selective solvent to the good one? Because we have known, for a single block copolymer PS-*b*-PB or PS-*b*-PMMA,[41−42] the preferential affinity of the good solvent for a certain block will induce significant changes in the morphology. Could the different preferential affinity of a good solvent for a

* To whom all correspondence should be addressed. E-mail: tbhe@ciac.jl.cn. Fax: +86-431-85262126. Phone: +86-431-85262123.
[†] Chinese Academy of Sciences.
[‡] Zhejiang University.

10.1021/ma701979q CCC: $40.75
Published on Web 12/29/2007

Table 1. Characteristics of the PS-*b*-PB Block Copolymers Used in This Work

sample	$M_{n,PS}$[a] $\times 10^{-3}$ (Da)	$M_{n,PB}$[a] $\times 10^{-3}$ (Da)	N[b]	w_{PS}[c]	f_{PS}[d]	M_w/M_n
S_1B_1	37.3	99.8[e]	2207	0.272[f]	0.241	1.002
S_2B_2	63.5	33.0	1222	0.658	0.621	1.09
S_3B_3	28.0	60.0	1380	0.318	0.284	1.19

[a] $M_{n,k}$, number-average molecular weight of the PS or PB. [b] N, total number-average degree of polymerization of the diblock. [c] w_{PS}, PS weight fraction. [d] f_{PS}, volume fraction of the PS block calculated from $f_{PS} = (w_{PS}/\rho_{PS})/((w_{PS}/\rho_{PS}) + (1 - w_{PS})/\rho_{PB})$ by using the following densities for the PS and PB blocks: $\rho_{PS} = 1.05$ g cm^{-3} and $\rho_{PB} = 0.895$ g cm^{-3}. [e] Total M_n determined from GPC data. [f] Determined by ^{13}C NMR spectral analyses.

Table 2. Characteristics of the Blend Systems of SB Block Copolymer

SB_x/SB_y	w_x/w_y[a]	Φ_{PS}[b]	Φ_x[c]	r[d]
S_1B_1/S_2B_2	20/80	0.541	0.210	1.806
S_1B_1/S_2B_2	33/67	0.490	0.347	1.806
S_1B_1/S_2B_2	50/50	0.427	0.501	1.806
S_1B_1/S_2B_2	67/33	0.365	0.676	1.806
S_1B_1/S_2B_2	80/20	0.313	0.811	1.806
S_3B_3/S_2B_2	50/50	0.449	0.501	1.129

[a] Weight fraction ratio in the blend systems. [b] Φ_{PS}, volume fraction of PS in the blend systems. [c] Φ_x, volume fraction of SB_x in the blend systems. [d] r, the ratio of the total number-average degree of polymerization of the two diblocks.

certain block still lead to different morphologies in the blend bcp thin film systems?

To address the above questions, the blend systems used in this work were the mixture of two asymmetric poly(styrene-*b*-butadiene) diblock copolymers, which had similar molecular weights but opposite spontaneous curvature and only the microphase separation had occurred in such blend systems.[19] Three different solvents, namely, heptane, cyclohexane, and benzene, corresponding to PB-selective, PB-preferential affinity, and PS-preferential affinity, respectively, were chosen as the annealing solvents. The effect of the nature of the annealing solvent on the morphology of the bcp blend thin film was investigated from a thermodynamic and kinetic origin, respectively.

Experimental Section

Materials. Three poly(styrene-*b*-butadiene) (SB) diblock copolymers coded as S_1B_1, S_2B_2, and S_3B_3 were purchased from Polymer Source Inc. Some characteristics of these block copolymers are summarized in Table 1. On the basis of the composition of each block copolymer, S_1B_1 and S_3B_3 are expected to form polystyrene (PS) cylinders in the polybutadiene (PB) matrix, while S_2B_2 is expected to form PB cylinders in the PS matrix. The block copolymers were separately dissolved in toluene to obtain the solutions with a certain concentration. S_1B_1/S_2B_2 mixtures with various weight fractions and a S_3B_3/S_2B_2 mixture with weight fraction ratio of 50/50 were then prepared. The details of these mixtures are shown in Table 2. The concentration of the blend solutions was 5 mg/mL if it was not pointed out specifically. It must be noted that the blend samples studied here were mixed at a molecular level regardless of the compositions of the mixing solutions.[19]

Sample Preparation. The thin films of the blend samples were spun cast onto the carbon-coated mica from the toluene solution at 2000 rpm for 30 s. The thickness of the as-cast thin films was approximately 40 nm for the 5 mg/mL blend solutions measured by D8 X-ray reflectometry. The samples were then directly put into an airtight vessel (approximately 31 cm^3) containing a reservoir of the annealing solvent. The characteristics of the annealing solvents are listed in Table 3. By varying the amount of solvent in the reservoir, the vapor pressure of the solvent in the airtight vessel

Table 3. Characteristics of the Annealing Solvents

	solubility parameter[a] δ (J/cm^3)$^{1/2}$	molar volume[b] V (mL/mol)	boiling temperature[c] T_b (°C)	viscosity (at 20 °C) η (cps)
benzene	18.8	88.9	80	0.520[a]
cyclohexane	16.8	108.0	81	0.979[a]
heptane	15.1	146.6	98	0.409[c]

[a] Obtained from Polymer Handbook. [b] Obtained from Properties of Polymers. [c] Obtained from Solvents Handbook.

Table 4. Vapor Pressures of the Annealing Solvents at Different Temperatures

benzene		cyclohexane		heptane	
temp[a] (°C)	vapor pressure (mmHg)	temp[a] (°C)	vapor pressure (mmHg)	temp[a] (°C)	vapor pressure (mmHg)
15.4	60	14.7	60	22.3	40
26.1	100	25.5	100	30.6	60
42.2	200	42.0	200	41.8	100

[a] temp: temperature.

can be adjusted.[47] Note that the amount of solvent in the reservoir was much larger than that absorbed by the thin film. After being exposed to the solvent vapor for different times, the samples were removed from the vessel as quickly as possible and air-dried at room temperature. The influence of the solvent evaporation on the morphology during the air-drying process was checked by the freeze-drying method,[41] which means that the thin films were freeze-dried as soon as they were removed from the solvent ambience. No morphological changes were obtained in the thin films, compared with directly air-drying at room temperature, which indicated that the solvent evaporation has little effect on the final morphology in the present work. Therefore, the resulting microdomain structures after annealing can be preserved via the fast solvent removal. In addition, since the vapor pressure during the annealing process could influence the microstructure,[48] the annealing temperature was controlled at 42 °C for heptane to ensure a similar saturated vapor pressure with those of cyclohexane and benzene at room temperature. Table 4 lists the vapor pressure of the annealing solvents at different temperatures.

Instruments. TM-AFM measurements were carried out on a NanoScope IIIa scanning probe microscope (Digital Instruments Inc.). During imaging, the AFM cantilever (spring constant between 1.5 and 3.5 N/m) was driven to oscillate at ~400 kHz, close to the cantilever's resonant frequency. The microscope was operated at the moderate tapping mode so that the glassy PS domains would appear as dark regions and the rubbery PB domains as bright regions in the phase images.[40]

TEM experiments were performed on a JEOL 1011 TEM with an accelerating voltage of 100 kV in the bright-field mode. For plain-view TEM studies, the thin film and its carbon support were floated off onto a pool of distilled water and then picked up with copper grids. To enhance the contrast between the PS and PB phases, the specimens were stained with osmium tetraoxide (OsO_4) for hours prior to observation. Since OsO_4 selectively reacted with the double bonds of the PB blocks, the PB phase would appear as a dark area and the PS phase as a bright area in the TEM micrographs. For cross-sectional TEM experiments, some portions of the floated film were collected onto a piece of cured epoxy resin and dried. After staining with OsO_4, these epoxy pieces were embedded in the epoxy resin and subsequently heated to 35, 45, and 55 °C, respectively, for 12 h. The ultrathin sections with approximately 50 nm thickness were microtomed using a LEICA Ultracut R microtome and a glass knife at room temperature and collected onto the carbon-coated copper grids.

The saturated time and the polymer concentration in the thin films, corresponding to the response of the thin films to certain vapor pressures of the annealing solvent, were measured by quartz crystal microbalance (Q-Sense AB) with the dissipation mode (QCM-D). The specimen of the thin film was spun cast onto the

Scheme 1. Morphologies Transition of the S_1B_1/S_2B_2 (50/50) Blend Thin Film as a Function of Time in the Different Saturated Vapor of Annealing Solvent

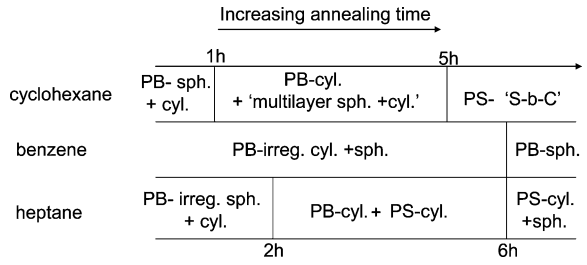

surface of the QCM-D sensor. The solvent vapor stream was taken into the QCM cell with controlled N_2 under a certain velocity of flow. (The vapor pressure of the solvent can be calculated). During the experiment, the temperature of the gas stream and cell was controlled. The fundamental resonant frequency was 5 MHz, and the constant (C) of the crystal used was 17.7 ng/cm^2. The Sauerbrey equation was used to measure the mass (Δm) of the samples and the over tone was chosen as 3.

Results and Discussion

The previous investigations for the phase behavior of block copolymer thin films annealed in the solvent vapor mainly focus on the "selective" solvent for the neat system.[39,49,50] The current investigation examines the effect of the "nonselective" solvent on the morphology transition of the thin films of blend block copolymer (bcp) systems.

Scheme 1 summarizes the microdomain structures of the blend thin film of S_1B_1/S_2B_2 with a weight fraction ratio of 50/50 as a function of annealing time in the saturated vapor of different solvents. In the vapor of heptane, the structure of irregular PB spheres and short PB cylinders in the PS matrix was first formed in the thin film. As the annealing time prolonged, the PB spheres and short cylinders fused to form the longer PB cylinders, while the PS phase tended to segregate. Finally, the PB phase formed the matrix and the PS phase was separated into cylinders and spheres. In the vapor of benzene, the thin film also showed the structures of irregular PB cylinders and spheres in the PS matrix at the initial annealing stage. The fraction of PB spheres increased with the annealing time, and the film exhibited the morphology of PB spheres dispersed in the PS continuum phase finally. For the thin film annealed in the cyclohexane vapor, the morphology evolution was a little complicated and an interesting "spheres-between-cylinders" structure (marked as PS−'S-b-C' in Scheme 1, which was discussed later) was observed after a certain annealing time.

The whole process of solvent annealing can be divided into two parts by the "saturated" state of the film. Before saturation, the solvent molecules penetrate into the film continually and the swollen extent of the thin film is increasing with the annealing time prolonged. The rearrangement of the blocks in the films is concurrent. After saturation, the diffusion of the solvent molecules into and out of the thin film reach equilibrium and the thin film is fully swollen. The blocks will keep reconstructing in the solvent ambience. The nature of the annealing solvent will strongly influence both of these processes. Not only the property of the solvent determines the saturated time and the swelling extent of the thin film but also affects the rearrangement of each block due to how "good" the solvent is for the polymer.

Annealing in the Saturated Vapor of Different Solvents. For a given polymer, there are good solvents, a (near) Θ solvent, and a nonsolvent. The polymer can be well dissolved in a good solvent but not in a nonsolvent. In a (near) Θ solvent, the polymer chains adopt a similar conformation of the ideal chains. The thermodynamic properties of the polymer solvent then depend on how "good" the solvent is for the polymer as well as on the polymer itself.[51] For a block copolymer, a solvent which is good for one block can be classified as a neutral, slightly selective, or strongly selective solvent, depending on whether it is a good, (near) Θ, or nonsolvent for the other block. The relative affinity of the solvent is governed by the polymer−solvent interaction parameter, $\chi_{P-S} = V_S(\delta_S - \delta_P)^2/RT + 0.34$,[52] where V_S is the molar volume of the solvent, R is the gas constant, T is the temperature, and δ_S and δ_P are the solubility parameters of the solvent and polymer, respectively. The solubility parameters for PS and PB are $\delta_{PS} = 18.6$ (J/cm^3)$^{1/2}$ and $\delta_{PB} = 17.0$ (J/cm^3)$^{1/2}$, respectively.[53] The polymer−solvent interaction parameters (χ) for different pairs of polymers and solvents under the annealing temperature are calculated and listed in Table 5. According to the Flory−Huggins criterion, cyclohexane is a good solvent for PB block and a (near) Θ solvent for PS block. Benzene is a good solvent for both PS and PB blocks but has preferential affinity for PS blocks. Heptane is a selective solvent for PB blocks.

Table 5. Interaction Parameters (χ) of the Polymer−Solvent at the Annealing Temperature

	benzene[a]	cyclohexane[a]	heptane[b]
PS	0.3414	0.5322[c]	1.0236
PB	0.4563	0.3417	0.5414

[a] Calculated from $\chi = V_s(\delta_s - \delta_p)^2/RT + 0.34$ at the annealing temperature 25 °C. [b] Calculated at the annealing temperature 43 °C. [c] Cyclohexane is a near Θ solvent for PS at 34.5 °C, $\chi_{PS-cyclohexane} = -0.556 + 324.3/T$.

Figure 1 shows the TEM micrographs of the final, unchangeable morphologies of the thin films after annealing in the saturated vapor of different solvents for 12 h. Note that the blend thin films will be totally swollen and saturated within 100∼200 min upon exposure to the vapor of three annealing solvents as indicated by quartz crystal microbalance (QCM-D) measurements. Therefore, Figure 1 presents the structures of the blend bcp thin films after fully swollen by the solvents.

The as-cast thin film of S_1B_1/S_2B_2 (50/50) showed the disorder morphology (Figure 1a). After annealed in heptane vapor for 12 h, the thin film generated the morphology of coexistent in-plane PS cylinders and PS spheres in the PB phase (Figure 1b). The average diameters of the PS cylinders and the PS spheres were approximately 33 ± 1 nm. When annealed in benzene vapor, the structure of PB spheres arraying within the continuous PS phase was observed (Figure 1c). The diameter of the PB spheres was approximately 46−52 nm. If the specimen was swollen in cyclohexane vapor for 12 h, the in-plane view of the blend thin film showed the morphology of bright PS spheres regularly arranging between PS cylinders (Figure 1d). The average diameters of the PS spheres and the PS cylinders were approximately 30.5 ± 3.5 nm and 24.3 ± 2.3 nm, respectively, and the average domain space between two PS cylinders was approximately 34.3 ± 2.6 nm. Parts e-A and e-B of Figure 1 show the cross-sectional view of the same thin film in Figure 1d along two different directions marked as A and B to clarify this structure further. (Note that the surface energy of PB is smaller than that of PS. A thin PB layer covered the free surface of the thin film with approximately 0.97 nm.) These two directional views were obtained by many microtome experiments along different cutting directions. Since the structure formed in the films was regular and the dimensions of the domains were uniform, we could judge the cut direction

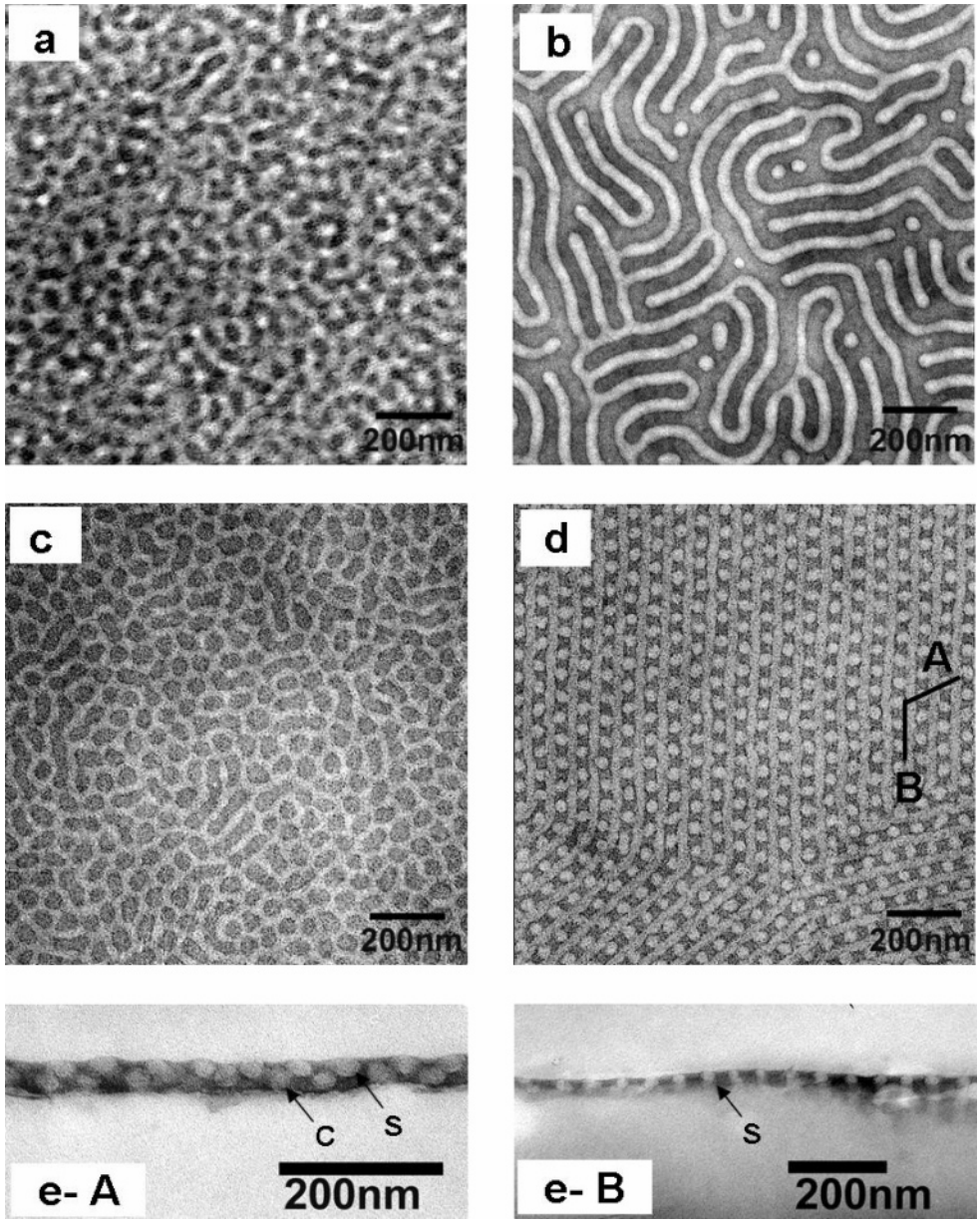

Figure 1. TEM morphologies of the S_1B_1/S_2B_2 (50/50) blend thin films spin-coated from a 5 mg/mL toluene solution annealed 12 h in the saturated vapor of different solvents: (a) the as-cast film; (b) heptane; (c) benzene; (d) cyclohexane; $(e)_{A,B}$ the cross-sectional views of the same thin film in part d along two directions marked as A and B.

compared with the dimension of the in-plane results. The TEM micrographs listed in parts d and e of Figure 1 showed that the PS phase in the thin film consisted of the in-plane cylinders and independent spheres (not the perpendicular cylinders as indicated by the black arrows in Figure 1e). Interestingly, the PS spheres regularly distributed between the PS cylinders. Therefore, such a structure shown in Figure 1d was named as "spheres-between-cylinders" (sph-b-cyl). Moreover, the bottom of the blend thin films also showed the "sph-b-cyl" structures (data not shown), which implied that the structure was formed in the entire film. In addition, the parallel annealing experiment was also carried out for the neat diblock copolymers of S_1B_1 or S_2B_2, respectively, and no such structure was observed in the thin films of neat systems.

Although the in-plane view of the "sph-b-cyl" structure is similar to the morphologies obtained by Jiang and Asari[13] and the structure simulated by Ping et al.,[54] they are completely different. Not only are the structures in these reported works all composed of three different kinds of blocks, but also the interaction of hydrogen bonding between the components of the blend systems[13] or chemical bond between the ABC triblocks[54] are found important for the morphology forming. For the "sph-b-cyl" structure, however, only two kinds of blocks, PS and PB, are included. No additional interactions, such as chemical bond or hydrogen bonding, exist between the two SB components.

Since heptane is a selective solvent for PB blocks, the heptane molecules tend to stay in the PB domain. Hence, the PB blocks may have more chance to relax and take the stretch configuration, while the PS blocks tend to aggregate to minimize the contacts with the solvent and the free energy of the thin films. As a result, the PB blocks will form the matrix phase of the thin films, while the PS blocks form the in-plane cylinders or spheres as in the vapor of heptane. It is worth to mention that we do not observe similar multilayer structures as reported by Chen et al.[30] when the thin film also annealed in a selective solvent. The possible reason may be that the different nature of selective solvents leads to a different extent of interaction

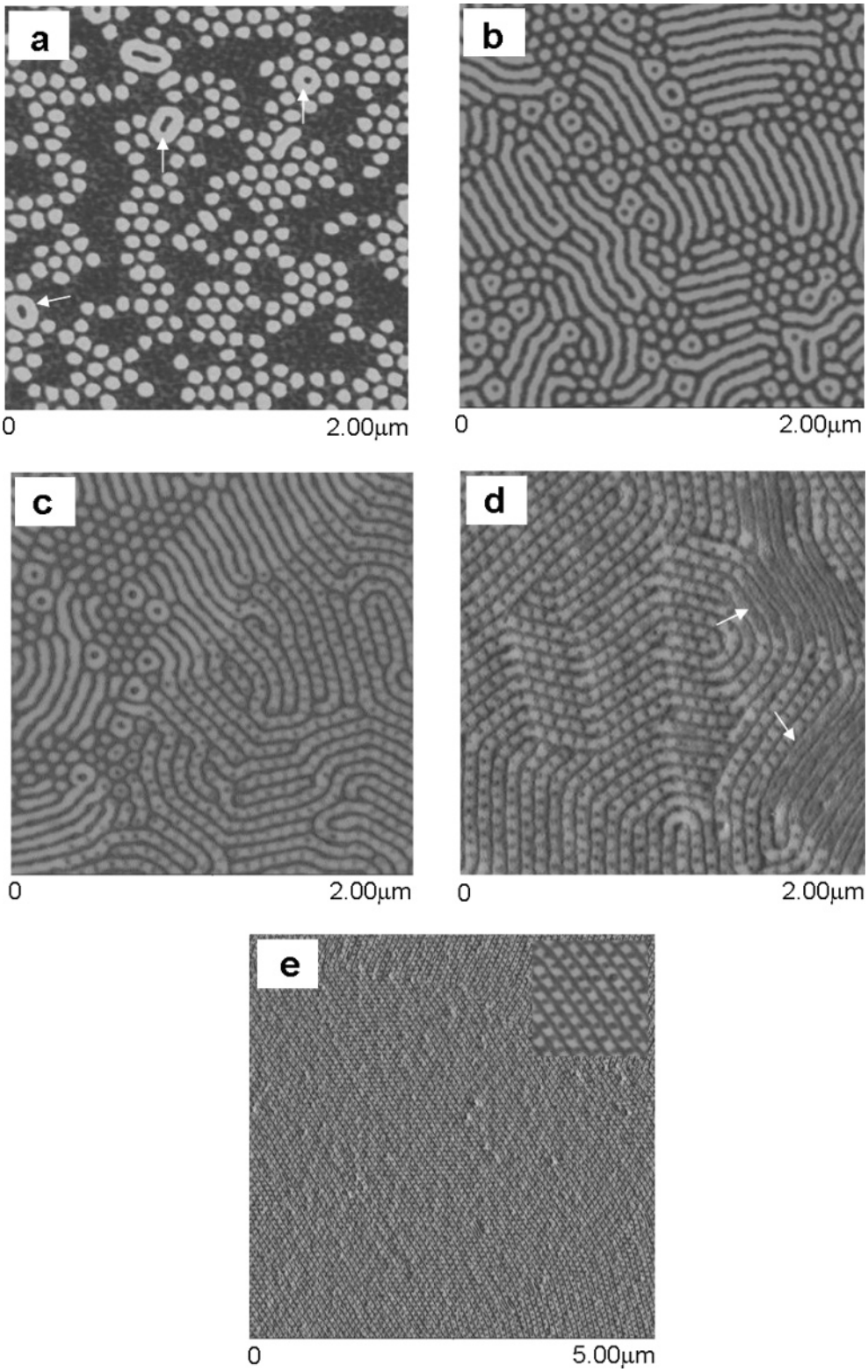

Figure 2. Tapping mode AFM phase images of S_1B_1/S_2B_2 (50/50) blend thin films annealed in the saturated vapor of cyclohexane for (a) 0.5 h, (b) 2 h, (c) 3 h, (d) 5 h, and (e) 12 h, respectively. The inset of part e is a local magnification image.

between the solvent and each block, which may affect the mobility and arrangement of the blocks in thin films.

With the change of the annealing solvent from a selective one to a good solvent, in the vapor of benzene, both PS and PB blocks can reconstruct themselves more freely. However, benzene has preferential affinity for PS blocks. Such a difference in the polymer−solvent interaction will make the diffusion rate of the solvent molecules in the PS phase slower than that in the PB phase. That means, compared with PB blocks, the PS blocks have more time to rearrange themselves under the same annealing condition. Therefore, the PS blocks tend to form the matrix phase, and the PB blocks will oppositely take the compact microdomain structure, although the compact extent of the PB blocks in this case is less than that of the PS blocks in heptane.

If the annealing solvent has preferential affinity for PB blocks, in the vapor of cyclohexane, the "sph-b-cyl" structure was observed. The preferential affinity of cyclohexane for PB blocks makes the PB blocks form the continuum matrix phase.

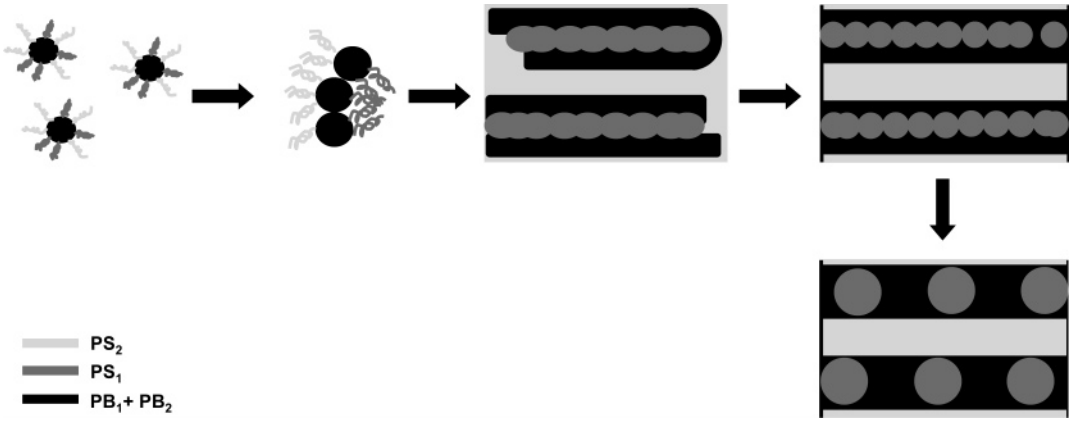

Figure 3. The schematic illumination of the formation process of "sph-b-cyl" structures.

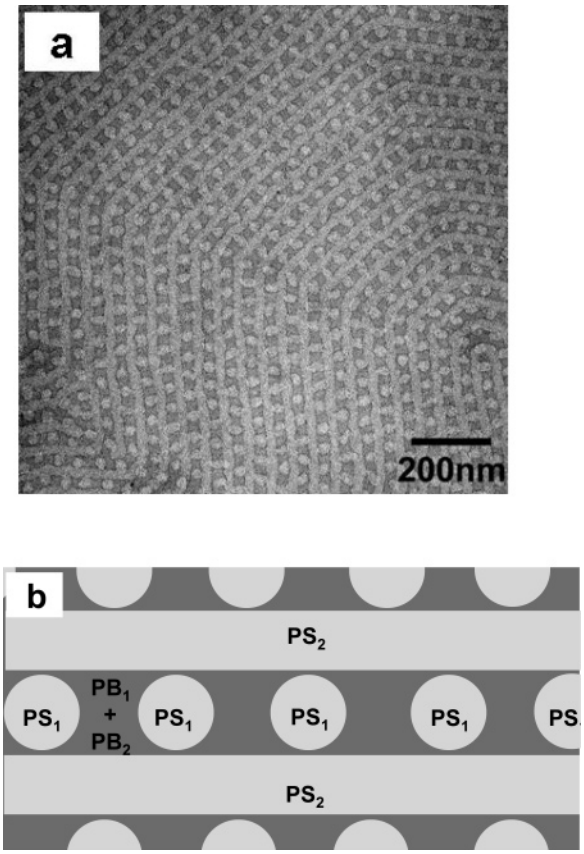

Figure 4. (a) TEM micrograph of the S_3B_3/S_2B_2 (50/50) blend thin film annealed in the saturated vapor of cyclohexane for 12 h. (b) The schematic representation of the disposition of the different PS blocks in the "sph-b-cyl" structure.

Nevertheless, compared with the case that PB blocks only form the spheres phase in the benzene vapor, the PS blocks in the films annealed by cyclohexane produce the alternate spheres and cylinders phase. The reason can be attributed to the large viscosity of cyclohexane contrasted with benzene (cf. Table 3). The large viscosity can further slow down the diffusion speed of solvent molecules and provides the PS blocks a relatively "long" time to relax as compared to benzene for PB blocks. Therefore, the PS blocks will rearrange to take their favorable morphologies in the vapor of cyclohexane, which resulted in the "sph-b-cyl" structure.

In fact the interfacial interactions, such as the free surface and substrate (shows a preference for one of the blocks) can influence the morphologies of the thin films greatly.[35−37] As has been shown, the PB block with the lower surface energy tends to segregate at the free surface which forms a thin layer (Figure 1e) in our observation. Therefore, besides the substrate of carbon-coated mica, the parallel experiments on the substrate of the silicon wafer were also performed, since PB preferentially wets silicon oxide, while the carbon coated mica surface is nearly neutral for both blocks.[36,55] However, the obtained morphologies did not show any significant difference between these two substrates after solvent annealing (date not shown). Therefore, the diversity morphologies studied here are mainly attributed to the different interactions between the blocks and solvent, and the influence of surface and interface will not be considered as a main factor to manipulate the different morphologies.

Morphologies under Different Annealing Conditions. Although the thermodynamic factor of the polymer−solvent interaction determined what kind of morphology was generated in the blend bcp films (as discussed above), it was found that the forming processes of such morphologies were also trapped by the kinetic factors.

Figure 2 shows the phase images of S_1B_1/S_2B_2 (50/50) thin films obtained by AFM as a function of annealing time in the saturated vapor of cyclohexane. After annealing 0.5 h, the thin film presented the morphology of dispersed PB spheres and short cylinders and some multilayered structures (indicated by the white arrows in Figure 2a), which was possibly developed by the fusion of the PB spheres and short cylinders. When extending the annealing time to 2 h (Figure 2b), more PB spheres and short cylinders were fused and connected with each other to form the multilayer structures. After annealing 3 h in the cyclohexane vapor, the "sph-b-cyl" structure appeared in part of the regions of the blend thin film (Figure 2c), i.e., some PS blocks form the independent spheres regularly arraying between the PS cylinders. In this crossover regime, the dimension of PS spheres was smaller than that of the final "sph-b-cyl" structure. Furthermore, besides the "sph-b-cyl" morphology, some PB spheres and cylinders still existed in the film. When the annealing time was prolonged to 5 h, most parts of the thin film produced the regular "sph-b-cyl" structures and only a few areas showed an "unfinished" state indicated by the white arrows in Figure 2d. After being exposed for 12 h, the whole film finally exhibited the regular "sph-b-cyl" structures as shown in Figure 2e. The cartoon simulation of the above evolution of the morphologies is presented in Figure 3.

Before we discuss the above results in more detail, we shall elucidate the effect of residual toluene on the morphology of the bcp blend thin films. Since the as-cast film was directly used for solvent treatment, there was some residual toluene solvent at the initial stage of solvent annealing. Although toluene

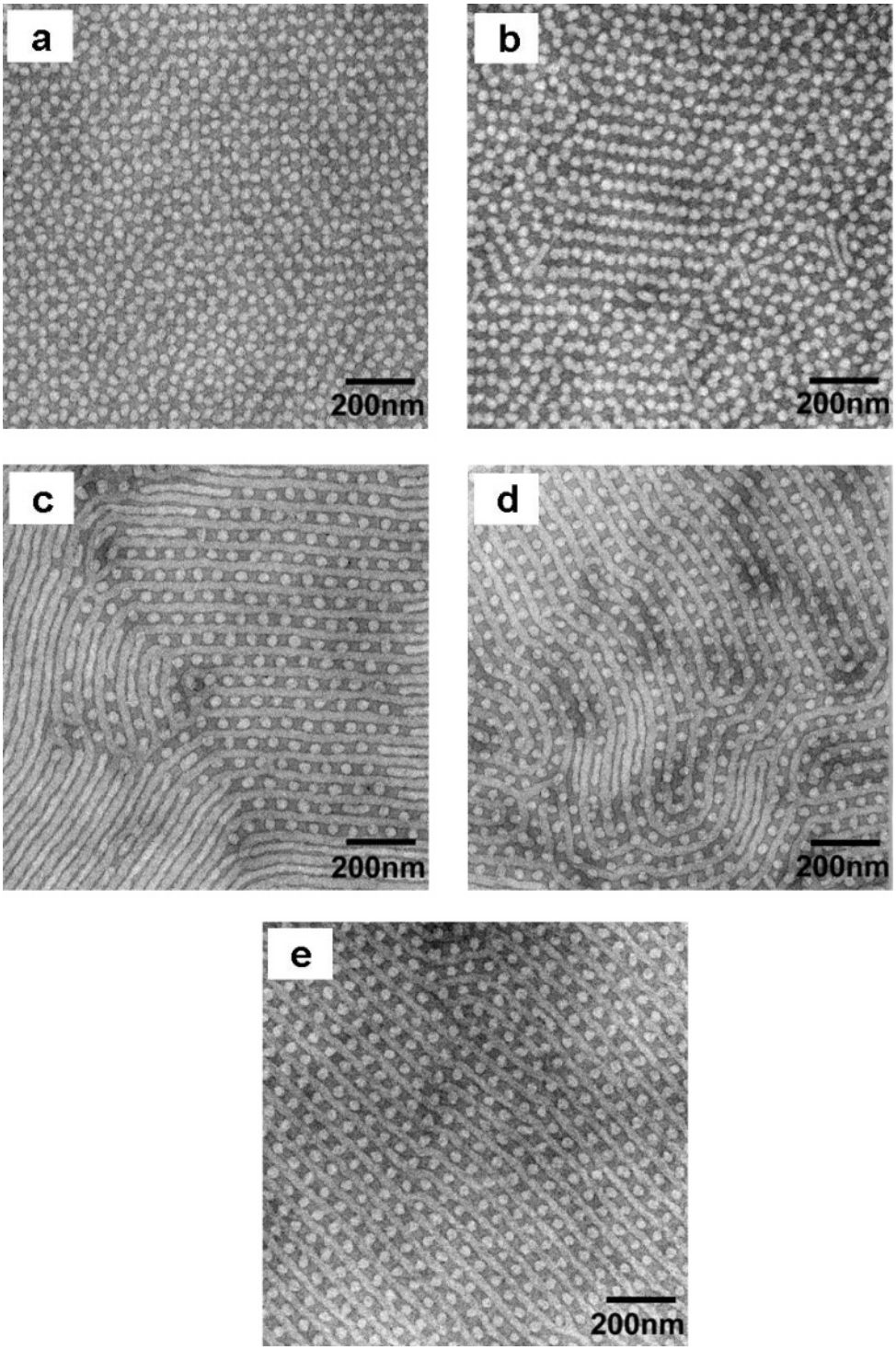

Figure 5. TEM morphologies of S_1B_1/S_2B_2 (50/50) blend thin films annealed in various vapor pressures of cyclohexane for 12 h. The vapor pressure was controlled by varying the amount of solvent in the reservoir: (a) 87, (b) 109, (c) 123, (d) 139, and (e) 185 μL.

is a good solvent for both PS and PB, it has a slight preferential affinity for PS blocks. Therefore, the PS blocks will move around the PB blocks preferentially, while the PB blocks take the aggregated form at the initial stage according to the first part of the discussion. Controlled annealing experiments were also carried out in the films by removing the residual toluene completely; the morphologies obtained obviously lacked ordering (data not shown) and were completely different from those observed in as-cast thin films. The results suggested that the residual toluene is necessary for the formation of various morphologies obtained here. The possible reason is that the residual toluene solvent makes the segments of the block copolymer chains possess a certain mobility at the initial stage of solvent treatment. Similar phenomena were also observed in the cases of benzene and heptane treatment (cf. Scheme 1).

When exposed to cyclohexane vapor, as the annealing time prolonged, more and more cyclohexane molecules will diffuse into the thin film and finally reach the saturated state. The preferential affinity of the cyclohexane will then play an important role leading to the PB blocks having more time to reconstruct. The dispersed PB microdomains tend to fuse together, while the PS domains prefer to separate from each other. Since the different length of the PS block of S_1B_1 (PS_1)

and S_2B_2 (PS_2) make them difficult to enter the same microdomain, the PS_1 and PS_2 will segregate and form their own microdomains, respectively. The blend interface will curve to the PS_1 phase due to the radius of the spontaneous interfacial curvature of S_1B_1 being smaller than that of S_2B_2, and then the multilayered structures are generated. With a further increase of the annealing time, the PB blocks tend to form the continuum phase due to the preferential affinity of cyclohexane, while the PS_1 and PS_2 blocks mainly form the dispersed in-plane cylinders. After annealing for enough time, possibly because of the different segregation strength induced by the different molecular weights[56] of the two PS blocks, the PS_1 cylinders break up into the spheres and attain a uniform distribution while the PS_2 blocks maintain the cylinders phase finally.

To testify to the above judgment of the disposition of the PS blocks in the "sph-b-cyl" structure, another system of S_3B_3/S_2B_2 (50/50) was employed. After the same annealing treatment in the cyclohexane vapor for 12 h, the S_3B_3/S_2B_2 blend thin film generated the similar "sph-b-cyl" structure with a different domain scale, as shown in Figure 4a. The average diameter of the PS in-plane cylinders was about 22.5 ± 1.3 nm, similar to that obtained in Figure 1d. However, the average diameter of the PS spheres was reduced from 30.5 ± 3.5 nm (Figure 1d) to 24.2 ± 2.0 nm (Figure 4a). The space between the two in-plane cylinders also changed from 34.3 ± 2.6 nm to 30.8 ± 1.5 nm. Both of the S_1B_1/S_2B_2 (50/50) and S_3B_3/S_2B_2 (50/50) systems have the same component of S_2B_2 and the approximate value of Φ_{PS}. The main difference is that the molecular weights of the PS and PB blocks in S_3B_3 are smaller than that in S_1B_1. After comparison of the changed domain dimension between Figures 1d and 4a, it can be concluded that the PS cylinders are made up with PS_2 blocks, while the PS_1 blocks form the PS spheres in the "sph-b-cyl" structure. Moreover, the volume fraction of the PS cylinders and the PS spheres in the "sph-b-cyl" structure are calculated from the TEM image to be approximately 25.3% and 10.8% for S_1B_1/S_2B_2 (50/50), which are also close to the theoretical values for the volume fractions of the PS_2 and PS_1 blocks, i.e., 30% and 12%, respectively. Therefore, the judgment of the disposition of the PS blocks related to the formation process of the "sph-b-cyl" structure is reasonable. Figure 4b schematically represents the disposition of the PS blocks in the "sph-b-cyl" structure of S_1B_1/S_2B_2 (50/50) blend thin films.

Besides the annealing time, the vapor pressure of the solvent in the annealing process also plays an important role in the morphology. Figure 5 shows the TEM images of S_1B_1/S_2B_2 (50/50) blend thin films annealed 12 h at different vapor pressures of cyclohexane. The vapor pressure was controlled by varying the amount of cyclohexane in the reservoir from 87, 109, 123, and 139 μL to 185 μL. (For cyclohexane, it would be the saturated vapor pressure at the room temperature, if the amount of solvent in the reservoir was more than 183 μL.)

After annealed in the vapor produced by 87 μL cyclohexane, a so-called "flower-like" pattern, which is comprised of six PS spheres and each PS sphere belongs to three "flowers", was observed (Figure 5a). It is similar to the result obtained by Peng et al.[49] The dimension of the spheres was uniform with the average diameter approximately 27.8 ± 2.3 nm. The "flower" patterns would become irregular and some PS spheres fuse together to form the short in-plane cylinders if the vapor pressure was produced by 109 μL of cyclohexane (Figure 5b). After exposure to the vapor produced by 123 μL of cyclohexane, the "flower-like" structures no longer exists; instead, the "sph-b-cyl" structure, together with some discontinuous in-plane PS cylinders, was formed (Figure 5c). The average diameters of the continuous in-plane cylinders and the spheres were 24.6 ± 1.0 nm and 29.5 ± 2.3 nm, respectively. When the amount of cyclohexane in the reservoir was increased up to 139 and 185 μL, the discontinuous short cylinders tended to disappear and the regular arranged "sph-b-cyl" structures appeared (parts d and e of Figure 5).

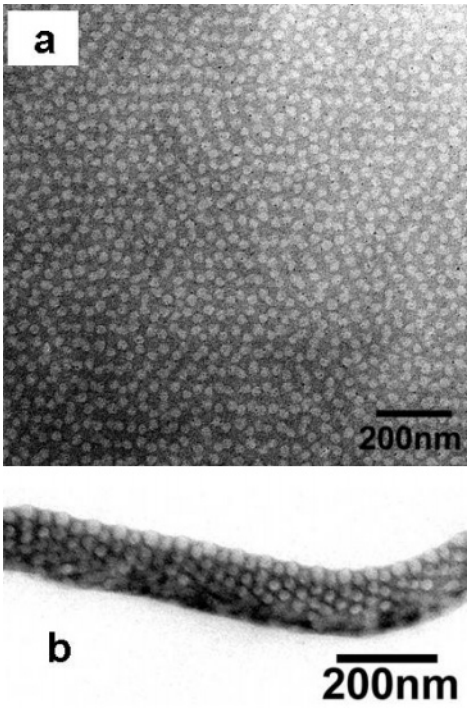

Figure 6. TEM morphologies of S_1B_1/S_2B_2 (50/50) blend thin films annealed in the saturated vapor of cyclohexane for 12 h. (a) In-plane view of the film spin-coated from the solution with a concentration less than 2.5 mg/mL, (b) cross-sectional view of the film spin-coated from a 10 mg/mL solution.

As reported, Knoll et al.[48] have investigated the morphology of SBS thin films under the controlled vapor pressure p of the annealing solvent. They pointed out that a different vapor pressure will lead to a different polymer concentration Φ_p in the films after totally swollen, which affects the thin film structures further. The relation between the normalized vapor pressure p/p_0 and the polymer volume fraction Φ_p is given as below.

$$\ln(p/p_0) = \mu_v/RT = \mu_s/RT = \chi_{p,s}\Phi_p^2 + \ln(1-\Phi_p) + (1-1/N)\Phi_p \quad (1)$$

N is the total degree of polymerization and $\chi_{p,s}$ is the Flory−Huggins interaction parameter between polymer and solvent, p_0 is the vapor pressure at saturation. Assuming that $\chi_{p,s}$ does not depend on Φ_p, $\chi_{p,s}$ of PS−PB/cyclohexne is approximately 0.3240 calculated with eq 1 as Φ_p measured by QCM-D measurements under a certain vapor pressure. Therefore, by increasing the amount of cyclohexane in the reservoir from 87 to 185 μL, Φ_p decreased from 83% to less than 30% according to eq 1. It is obvious that more solvent molecules penetrate inside the thin film; more chance for the blocks to arrange themselves into their favorable structures due to the relative "prolonged" time for relaxation. Moreover, if the partial volumes of polymer and solvent in the film are additive, Φ_p can be related to the film thickness via $\Phi_p = d_0/d_i$, where d_0 is the thickness of the dry films and d_i is the thickness of the fully swollen film in the solvent vapor. Since Φ_p is approximately 0.65 for

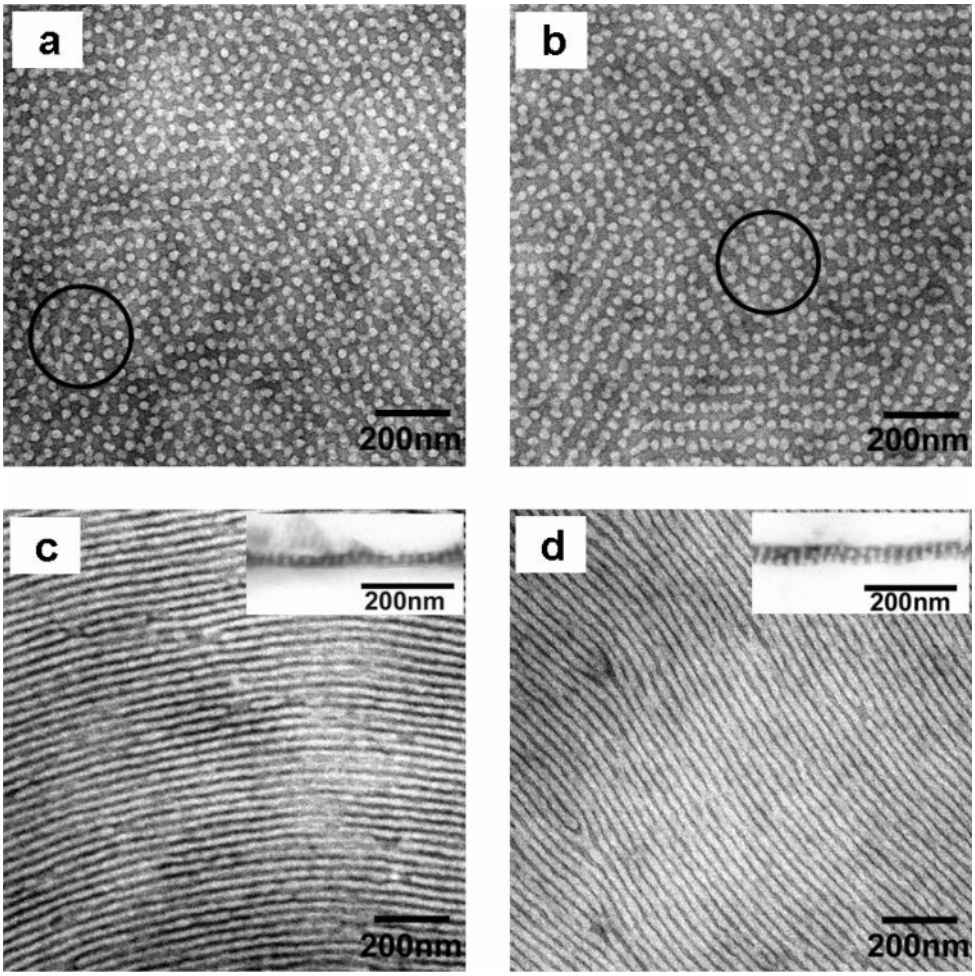

Figure 7. TEM morphologies of S_1B_1/S_2B_2 blend thin films with various compositions after annealed in the saturated vapor of cylcohexane for 12 h. The weight ratio of S_1B_1 and S_2B_2 are (a) 80/20, (b) 67/33, (c) 33/67, and (d) 20/80, respectively. The insets of parts c and d show the cross-sectional views of the thin films.

producing the regular "sph-b-cyl" structures in the blend thin films (corresponding to 139 μL of cyclohexane in the reservoir), the thickness of the swollen film d_i should be 62 nm if d_0 is 40 nm. It indicates that the formation of the "sph-b-cyl" morphology is related to the initial thickness d_0 of the blend thin film. If the initial thickness d_0 of the blend film was decreased by reducing the concentration of the blend solution, the regular "sph-b-cyl" structure in the blend thin film would gradually disappear even in the saturated vapor pressure. When the concentration of the blend solution was less than 2.5 mg/mL, no more regular "sph-b-cyl" structure was formed in the film (Figure 6a). On the contrary, if the thickness of d_0 was increased to 107 nm by using the spin solution of 10 mg/mL, the multilayer "sph-b-cyl" structure was formed in the perpendicular direction (Figure 6b).

It should be emphasized that all of these structures obtained in the thin films annealed by solvent would disappear after thermal treatment. Because the morphologies of the blend thin films were influenced greatly by kinetic factors as described above, we suggested that the structures obtained were the metastable state which is kinetically trapped by solvent treatment.

Effect of the Blend Composition. Hashimoto et al.[19,28,57] have investigated the thermodynamic equilibrium structures of the similar binary systems in bulk. They pointed out that when mixing two diblock copolymers, polystyrene-*b*-polyisoprene (SI), which have opposite spontaneous curvature with equal amounts, the mixture will show a lamellar structure at the equilibrium state if totally mixed at the molecular level. Feng et al.[57] also showed that the morphology of such a blend system SI_α/SI_β would change from the PS cylinder, lamella, and finally to the PI cylinder with increasing amount of β, which corresponds to an increase of the Φ_{PS} in the blend from 0.19 to 0.71. For thin film specimens, the transformation of the equilibrium states with varied Φ_{PS} for such systems has not been reported. Although we try to use the thermal treatment to explore the equilibrium state of the S_1B_1/S_2B_2 mixtures with various weight fractions in thin films, unfortunately, no long-range structures have been observed in the present experiment (data not shown). However, when we annealed the blend bcp thin films in certain solvent vapors, different long-range metastable structures were generated as Φ_{PS} changed.

Figure 7 shows the morphologies of S_1B_1/S_2B_2 blend thin films with various weight fractions annealed in the saturated vapor of cyclohexane for 12 h. Both S_1B_1/S_2B_2 (80/20) and S_1B_1/S_2B_2 (67/33) thin films presented the sphere collective morphologies which formed irregular "flower-like" patterns (as indicated by the black circles in Figure 7a,b). Since the PS blocks of the two block copolymers would, respectively, form their own microdomain, the diameters of the PS spheres were not uniform, leading to the irregular "flower-like" structures. It should be note that the "flower-like" structures formed here were different from the structure observed in Figure 5a. Since the structure shown in Figure 5a was generated under the lower vapor pressure and only a few cyclohexane molecules would penetrate into the film, in such a case the driving force may

not be enough for the PS blocks to separate and form their own microdomain. Therefore, the dimension of the spheres in Figure 5a was uniform and the "flower-like" pattern was regular.

In contrast with the morphology of S_1B_1/S_2B_2 (80/20) (Figure 7a), the "flower" pattern in the thin film of S_1B_1/S_2B_2 (67/33) (Figure 7b) was loose and tended to disappear. When the weight fraction of S_1B_1/S_2B_2 was 50/50, the regular "sph-b-cyl" structure formed (Figure 1d). With an increase in the amount of the S_2B_2 component further, in the systems of S_1B_1/S_2B_2 (33/67) and S_1B_1/S_2B_2 (20/80), the morphologies of in-plane cylinders were observed in the blend thin films. The TEM images of the in-plane and cross-sectional view shown in Figure 7c,d evidently confirmed that the PS blocks formed the in-plane cylinder phase in the matrix of the PB phase.

Although the volume fractions of the PS block, Φ_{PS}, for these systems were only varied from 0.313, 0.365, 0.427, and 0.490 to 0.541, the various morphologies were observed in the blend thin films of S_1B_1/S_2B_2, which changed from PS spheres, PS spheres and cylinders ("sph-b-cyl") to PS cylinders in the PB matrix. The result indicated that the preferential affinity of the solvent for a certain block indeed has a significant effect on the morphology of blend thin films, which changes the effective volume fraction of that block and alters the interfacial curvature. As a result, the "response" of the morphology as Φ_{PS} changed is intensified.

Conclusions

The effects of solvent treatments on the morphologies of the blend thin films consisting of two PS-*b*-PB diblock copolymers, which have similar molecular weights but opposite spontaneous curvatures, were systematically investigated. The results reveal that even a slight preferential affinity of good solvent for one block will strongly alter the morphology of the blend thin films. After annealing in saturated heptane vapor for 12 h, which is a selective solvent for PB blocks, the morphology of the in-plane PS cylinders and PS spheres in the PB matrix was observed in the S_1B_1/S_2B_2 (50/50) blend thin film. When annealing in saturated benzene vapor, which is a good solvent for both blocks and has a preferential affinity for the PS block, the thin film shows a structure of PB spheres arraying within the PS matrix. An interesting structure of "spheres-between-cylinders" ("sph-b-cyl") can be formed in saturated cyclohexane vapor, which is a good solvent for PB and a (near) Θ solvent for PS at 34.5 °C and has a preferential affinity for PB blocks. The in-plane cylinders and spheres in the "sph-b-cyl" structure were found to be made up of different PS blocks of S_1B_1 and S_2B_2, respectively.

The kinetic factors such as the annealing time and solvent vapor pressure, together with the film thickness and the composition of the blend system, were found to strongly affect the morphologies of the blend thin films as well. Rich structures of the blend thin films have been obtained under various conditions. As an extreme model of A−B/A−C blends with no interactions between the B and C blocks, the results obtained in this work indicate that blending the block copolymers together with the solvent annealing is a noteworthy way to control the structure and morphology. Because block copolymer blends showed wide molecular weight distributions, it would be important for the application study.

Acknowledgment. We are grateful to Prof. Guangzhao Zhang and Mr. Yi Hou of University of Science and Technology of China for assistance with the QCM measurements and Ms. Guifen Sun for technical help with the microtomy. This work is supported by National Science Foundation of China (Grant 20774095) and subsidized by National Basic Research Program of China (Grant 2005CB6238). B. Du thanks the financial support of Zhejiang Provincial Natural Science Foundation of China (Grant Y406029).

References and Notes

(1) Hamley, I. W. *The Physics of Block Copolymers*; Oxford University Press: New York, 1998.
(2) Bates, F. S.; Fredrickson, G. H. *Phys. Today* **1999**, *52*, 32.
(3) Park, C.; Yoon, J.; Thomas, E. L. *Polymer* **2003**, *44*, 6725.
(4) Ruzette, A.; Leibler, L. *Nat. Mater.* **2005**, *4*, 19.
(5) Abetz, V.; Simon, P. F. W. *Adv. Polym. Sci.* **2005**, *189*, 125.
(6) Park, M.; Harrison, C.; Chaikin, P. M.; Register, R. A.; Adamson, D. H. *Science* **1997**, *276*, 1401.
(7) Thurn-Albrecht, T.; Schotter, J.; Kastle, G. A.; Emley, N.; Shibauchi, T.; Krusin-Elbaum, L.; Guarini, K.; Black, C. T.; Tuominen, M. T.; Russell, T. P. *Science* **2000**, *290*, 2126.
(8) Jeong, U.; Kim, H.; Rodriguez, R. L.; Tsai, I. Y.; Stafford, C. M.; Kim, J. K.; Hawker, C. J.; Russell, T. P. *Adv. Mater.* **2002**, *14*, 274.
(9) Förster, S.; Antonietti, M. *Adv. Mater.* **1998**, *10*, 195.
(10) Lazzari, M.; López-Quintela, M. A. *Adv. Mater.* **2003**, *15*, 1583.
(11) (a) Erhardt, R.; Boker, A.; Zettl, H.; Kaya, H.; Pyckhout-Hintzen, W.; Krausch, G.; Abetz, V.; Mueller, A. H. E. *Macromolecules* **2001**, *34*, 1069. (b) Hayashida, K.; Takano, A.; Arai, S.; Shinohara, Y.; Amemiya, Y.; Matsushita, Y. *Macromolecules* **2006**, *39*, 9402. (c) Masuda, J.; Takano, A.; Suzuki, J.; Nagata, Y.; Noro, A.; Hayashida, K.; Matsushita, Y. *Macromolecules* **2007**, *40*, 4023.
(12) Goldacker, T.; Abetz, V. *Macromol. Rapid Commun.* **1999**, *20*, 415.
(13) (a) Jiang, S.; Gopfert, A.; Abetz, V. *Macromolecules* **2003**, *36*, 6171. (b) Asari, T.; Matsuo, S.; Takano, A.; Matsushita, Y. *Macromolecules* **2005**, *38*, 8811.
(14) Koneripalli, N.; Levicky, R.; Bates, F. S.; Matsen, M. W.; Satija, S. K.; Ankner, J.; Kaiser, H. *Macromolecules* **1998**, *31*, 3498.
(15) Birshtein, T. M.; Lyatskaya, Y. V.; Zhulina, E. B. *Polymer* **1992**, *33*, 2750.
(16) Shi, A.-C.; Noolandi, J. *Macromolecules* **1995**, *28*, 3103.
(17) (a) Matsen, M. W. *J. Chem. Phys.* **1995**, *103*, 3268. (b) Matsen, M. W.; Bates, F. S. *Macromolecules* **1995**, *28*, 7298.
(18) Rysz, J. *Polymer* **2005**, *46*, 977.
(19) (a) Hashimoto, T.; Yamasaki, K.; Koizumi, S.; Hasegawa, H. *Macromolecules* **1993**, *26*, 2895. (b) Koizumi, S.; Hasegawa, H.; Hashimoto, T. *Macromolecules* **1994**, *27*, 4371.
(20) Vilesov, A. D.; Floudas, G.; Pakula, T.; Melenevskaya, E. Y.; Birshtein, T. M.; Lyatskaya, Y. V. *Macromol. Chem. Phys.* **1994**, *195*, 2317.
(21) Spontak, R. J.; Fung, J. C.; Braunfeld, M. B.; Sedat, J. W.; Agard, D. A.; Kane, L.; Smith, S. D.; Satkowski, M. M.; Ashraf, A.; Hajduk, D. A.; Gruner, S. M. *Macromolecules* **1996**, *29*, 4494.
(22) Lin, E. K.; Gast, A. P.; Shi, A.-C.; Noolandi, J.; Smith, S. D. *Macromolecules* **1996**, *29*, 5920.
(23) Kane, L.; Satkowski, M. M.; Smith, S. D.; Spontak, R. J. *Macromolecules* **1996**, *29*, 8862.
(24) Zhao, J.; Majumdar, B.; Schulz, M. F.; Bates, F. S.; Almdal, K.; Mortensen, K.; Hajduk, D. A.; Gruner, S. M. *Macromolecules* **1996**, *29*, 1204.
(25) Sakurai, S.; Irie, H.; Umeda, H.; Nomura, S.; Lee, H. H.; Kim, J. K. *Macromolecules* **1998**, *31*, 336.
(26) Court, F.; Yamaguchi, D.; Hashimoto, T. *Macromolecules* **2006**, *39*, 2596.
(27) Mayes, A. M.; Russell, T. P.; Deline, V. R.; Satija, S. K.; Majkrzak, C. F. *Macromolecules* **1994**, *27*, 7447.
(28) Yamaguchi, D.; Hashimoto, T.; Han, C.; Baek, D.; Kim, J.; Shi, A.-C. *Macromolecules* **1997**, *30*, 5832.
(29) Green, P. F.; Limary, R. *Adv. Colloid Interface Sci.* **2001**, *94*, 53.
(30) Chen, Y.; Wang, Z.; Gong, Y.; Huang, H.; He, T. *J. Phys. Chem. B* **2006**, *110*, 1647.
(31) Morkved, T. L.; Lu, M.; Urbas, A. M.; Ehrichs, E. E.; Jaeger, H. M.; Russell, T. P. *Science* **1996**, *273*, 931.
(32) Funaki, Y.; Kumano, K.; Nakao, T.; Jinnai, H.; Yoshida, H.; Kimishima, K.; Tsutsumi, K.; Hirokawa, Y.; Hashimoto, T. *Polymer* **1999**, *40*, 7147.
(33) Thurn-Albrecht, T.; DeRouchey, J.; Russell, T. P.; Jaeger, H. M. *Macromolecules* **2000**, *33*, 3250.
(34) Fukunaga, K.; Elbs, H.; Magerle, R.; Krausch, G. *Macromolecules* **2000**, *33*, 947.
(35) Buck, E.; Fuhrmann, J. *Macromolecules* **2001**, *34*, 2172.
(36) Tsarkova, L.; Knoll, A.; Krausch, G.; Magerle, R. *Macromolecules* **2006**, *39*, 3608.
(37) Wang, Q.; Nealey, P. F.; de Pablo, J. J. *Macromolecules* **2001**, *34*, 3458.

(38) (a) Kim, G.; Libera, M. *Macromolecules* **1998**, *31*, 2569. (b) Elbs, H.; Drummer, C.; Abetz, V.; Krausch, G. *Macromolecules* **2002**, *35*, 5570. (c) Cavicchi, K. A; Russell, T. P. *Macromolecules* **2007**, *40*, 1181.
(39) Chen, Y.; Huang, H.; Hu, Z.; He, T. *Langmuir* **2004**, *20*, 3805.
(40) (a) Zhang, Q.; Tsui, O. K. C.; Du, B.; Zhang, F.; Tang, T.; He, T. *Macromolecules* **2000**, *33*, 9561. (b) Huang, H.; Zhang, F.; Hu, Z.; Du, B.; He, T.; Lee, F. K.; Wang, Y.; Tsui, O. K. C. *Macromolecules* **2003**, *36*, 4084.
(41) (a) Huang, H.; Hu, Z.; Chen, Y.; Zhang, F.; Gong, Y.; He, T.; Wu, C. *Macromolecules* **2004**, *37*, 6523. (b) Gong, Y.; Huang, H.; Hu, Z.; Chen, Y.; Chen, D.; Wang, Z.; He, T. *Macromolecules* **2006**, *39*, 3369.
(42) Gong, Y.; Hu, Z.; Chen, Y.; Huang, H.; He, T. *Langmuir* **2005**, *21*, 11870.
(43) Niu, S.; Saraf, R. F. *Macromolecules* **2003**, *36*, 2428.
(44) Radzilowski, L. H.; Carvalho, B. L.; Thomas, E. L. *J. Polym. Sci., Part B: Polym. Phys.* **1996**, *34*, 3081.
(45) Böker, A.; Müller, A. H. E.; Krausch, G. *Macromolecules* **2001**, *34*, 7477.
(46) Kim, S. H.; Misner, M. J.; Russell, T. P. *Adv. Mater.* **2004**, *16*, 2119.
(47) Zhu, J.; Zhao, J.; Liao, Y.; Jiang, W. *J. Polym. Sci., Part B: Polym. Phys.* **2005**, *43*, 2874.
(48) Knoll, A.; Magerle, R.; Krausch, G. *J. Chem. Phys.* **2004**, *120*, 1105.
(49) Peng, J.; Wei, Y.; Wang, H.; Li, B.; Han, Y. *Macromol. Rapid Commun.* **2005**, *26*, 738.
(50) Peng, J.; Han, Y.; Knoll, W.; Kim, D. *Macromol. Rapid Commun.* **2007**, *28*, 1422.
(51) Teraoka, I. *Polymer Solutions: An Introduction to Physical Properties*; John Wiley & Sons: New York, 2002.
(52) *Polymer Handbook*, 3rd ed.; Brandrup, J., Immergut, E. H., Eds.; John Wiley & Sons: New York, 1989.
(53) Pico, E. R.; Williams, M. C. *J. Polym. Sci., Phys. Ed.* **1977**, *15*, 1585.
(54) Tang, P.; Qiu, F.; Zhang, H.; Yang, Y. *Phys. Rev. E* **2004**, *69*, 031803.
(55) Harrison, C.; Park, M.; Chaikin, P. M.; Register, R. A.; Adamson, D. H.; Yao, N. *Polymer* **1998**, *39*, 2733.
(56) Epps, T. H., III; Bates, F. S. *Macromolecules* **2006**, *39*, 2676.
(57) Chen, F.; Kondo, Y.; Hashimoto, T. *Macromolecules* **2007**, *40*, 3714.

MA701979Q